

Current-induced torques and interfacial spin-orbit coupling

Paul M. Haney,¹ Hyun-Woo Lee,² Kyung-Jin Lee,^{1,3,4,5} Aurélien Manchon,⁶ and M. D. Stiles¹

¹Center for Nanoscale Science and Technology, National Institute of Standards and Technology, Gaithersburg, Maryland 20899-6202, USA

²Department of Physics, Pohang University of Science and Technology, Pohang, 790-784, Korea

³Department of Materials & Engineering, Korea University, Seoul 136-701, Korea

⁴KU-KIST Graduate School of Converging Science and Technology, Korea University, Seoul 136-701, Korea

⁵University of Maryland, Maryland Nanocenter, College Park, Maryland 20742 USA

⁶King Abdullah University of Science and Technology (KAUST), Physical Science and Engineering Division, Thuwal 23955-6900, Saudi Arabia

(Received 5 September 2013; published 19 December 2013)

In bilayer systems consisting of an ultrathin ferromagnetic layer adjacent to a metal with strong spin-orbit coupling, an applied in-plane current induces torques on the magnetization. The torques that arise from spin-orbit coupling are of particular interest. Here we use first-principles methods to calculate the current-induced torque in a Pt-Co bilayer to help determine the underlying mechanism. We focus exclusively on the analog to the Rashba torque, and do not consider the spin Hall effect. The details of the torque depend strongly on the layer thicknesses and the interface structure, providing an explanation for the wide variation in results found by different groups. The torque depends on the magnetization direction in a way similar to that found for a simple Rashba model. Artificially turning off the exchange spin splitting and separately the spin-orbit coupling potential in the Pt shows that the primary source of the “fieldlike” torque is a proximate spin-orbit effect on the Co layer induced by the strong spin-orbit coupling in the Pt.

DOI: 10.1103/PhysRevB.88.214417

PACS number(s): 85.35.-p, 72.25.-b

I. INTRODUCTION

Spintronics has had significant impact on information technology, the most common example being the read heads in hard disk drives. It is poised to have even greater impact, led by the development of devices such as spin transfer torque-based magnetic random access memory. A crucial component of this next generation of spintronic applications is the control of magnetic orientation with an electrical current^{1,2} (or electric field^{3,4}). The approach is furthest developed in magnetic tunnel junctions, which utilize spin transfer torque to reversibly switch the magnetization in one of the layers. An alternative approach has been demonstrated in recent experiments on bilayer systems consisting of ultrathin ferromagnetic layers adjacent to heavy metals such as Pt.⁵⁻¹³ In these systems, spin-orbit coupling is responsible for current-induced torques. There are indications that the efficiency of these current-induced torques (measured as, for example, the torque per current density) may be larger than the conventional spin transfer torque.¹⁴ For this reason among others, these bilayer and related systems offer a possible route for spintronics to fulfill its full promise in technological applications.

The spin-orbit coupling in these systems leads to multiple effects. For one, there is a spin Hall effect in the Pt layer, so that spin current flows from the Pt into the magnetic layer, with spin orientation perpendicular to the charge current direction and the interface normal. This spin current flux induces magnetization dynamics via the conventional spin transfer torque. A distinct effect originates from the simultaneous presence of magnetization, spin-orbit coupling, and broken inversion symmetry at the interface. These ingredients result in an electronic structure in which current carrying states acquire a spin accumulation transverse to the magnetization, resulting in a torque.¹⁵ Both the spin Hall effect and interfacial spin-orbit torque are proportional to the charge current.

An additional consequence of the interfacial spin-orbit coupling is the current-independent Dzyaloshinskii-Moriya (DM) interaction,¹⁶⁻¹⁸ which has been argued to be important^{11,12,19} for current-induced domain wall motion.

The vector components of the spin-orbit torques can be decomposed into two vector fields as a function of $\hat{\mathbf{M}}$, the magnetization direction: $\hat{\mathbf{M}} \times (\hat{\mathbf{J}} \times \hat{\mathbf{z}})$, which we refer to as a fieldlike torque and $\hat{\mathbf{M}} \times [\hat{\mathbf{M}} \times (\hat{\mathbf{J}} \times \hat{\mathbf{z}})]$, which we refer to as a dampinglike torque ($\hat{\mathbf{J}}$ is the charge current direction and $\hat{\mathbf{z}}$ is the interface normal).²⁰ These names derive from the similarity of the first form to the torque due to a field along $\hat{\mathbf{J}} \times \hat{\mathbf{z}}$, and the second to the damping that would result from precession around that field.

Depending on the assumed scattering processes, both the mechanism that combines the spin Hall effect plus spin-transfer torque and the interfacial mechanism can give torques in both directions.²¹⁻²⁴ However in the clean limit of the relaxation time approximation, Freimuth *et al.*²⁵ have shown that the physics behind two torque components separate rather cleanly: The damping torque originates predominantly from the spin Hall effect, and is a consequence of the perturbation of electronic states by the applied electric field, while the fieldlike torque originates mostly from the spin-orbit coupling at the interface, in conjunction with the perturbation of the electron distribution function by the applied field. In this paper, we focus on the underlying physics behind the interfacial spin-orbit torque, neglecting the spin Hall effect. In the terminology of Ref. 25, we only calculate the odd torque $\Gamma(\hat{\mathbf{M}}) = -\Gamma(-\hat{\mathbf{M}})$, and show that this component yields predominantly “fieldlike” torques for realistic systems (within the relaxation time approximation).

Which of these mechanisms is responsible for these current-induced torques is controversial. Measurements of the reversal of magnetic layers are interpreted in terms of a dampinglike torque due to the spin Hall effect.¹⁴ Some experiments on

current-induced domain wall motion in these systems are interpreted in terms of a dampinglike torque in combination with the DM interaction.^{11,12} Other experiments are interpreted in terms of a combination of fieldlike and dampinglike torques arising from the interface.⁵ Experimental measurements of the torque vector show varied results for the magnitude of the fieldlike and dampinglike torques, depending sensitively on the sample details.¹⁰ Calculations²⁵ show both torques to be present and sensitive to structural details. The spin-orbit coupling affects the magnetization dynamics in multiple ways, and clearly distinguishing the different contributions requires more careful experimental and theoretical efforts. In this work, we calculate the current-induced torques present at the interface between Co and Pt using first-principles methods. As discussed in Sec. II, we do not include the contributions from the spin Hall effect. The calculation is therefore analogous to that of the 2DEG Rashba model, but with the full electronic structure of the Co-Pt interface taken into account. With this approach, we explore the sensitivity of the current-induced torques to the system structure, the angular dependence of the current-induced torques, and attempt to identify the most important physical ingredients of the system which lead to the current-induced torques.

II. METHOD

A quantitative description of any system using density functional theory requires specific knowledge of the atomic structure. In the absence of experimental characterization at this level of detail, we study a variety of structures to reach qualitative conclusions. Our aim with this approach is to extract semiquantitative estimates of the current-induced torques, and to identify the trends and most important physical mechanisms underlying the current-induced torques.

There is significant mismatch between the lattice constants of bulk fcc Co and Pt ($a_{\text{Co}} = 0.354$ nm, $a_{\text{Pt}} = 0.392$ nm). Studies of Co growth on Pt observe a structure that is generally inhomogeneous and quite sensitive to the Co coverage.^{26,27} For simplicity, we assume a uniform Co layer with the in-plane Pt lattice constant.²⁸ The distance between interface Co and Pt layers is taken from Ref. 30, and the distance between Co planes was chosen to match the bulk Co density. Our qualitative conclusions do not depend sensitively on these choices, as we discuss in Sec. III. We present results for 1, 2, and 3 monolayers (ML) of Co on 8 layers of Pt, stacked along the [111] direction. We generally take the Co layer stacking to be fcc. We also study systems with an intermixed interface [see Fig. 1(b)]. Computational limitations preclude the use of super cells large enough to realistically describe such disorder; however the unit cells with intermixed interfaces do reduce the overall symmetry of the system.

We use the local spin density approximation,³¹ with full noncollinear spin, and include spin-orbit coupling using the on-site approximation as described in Ref. 32. We include 1.1 nm of vacuum along the \hat{z} direction and use a minimal localized atomic orbital basis set (a single s, p, d basis set for each atom) and norm-conserving pseudopotentials. Adequately converging the ground state energy requires a 2D k -point mesh with mesh spacing $dk = 0.18$ nm⁻¹.

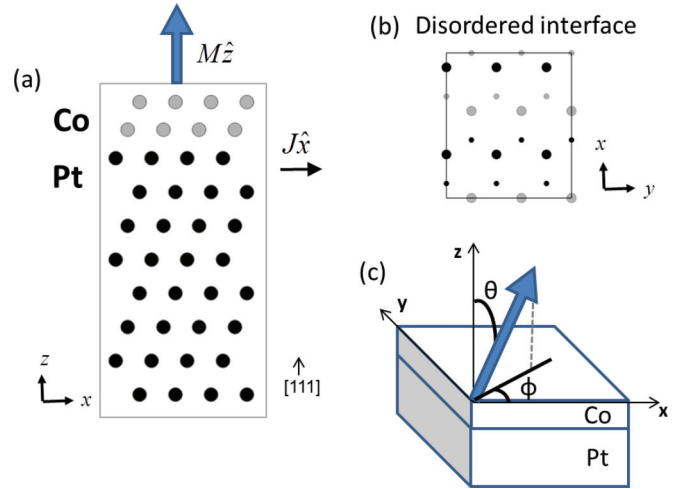


FIG. 1. (Color online) (a) System geometry for an ideal interface. (b) Example of an alloyed interface. Black (gray) dots represent Pt (Co), and the larger dots are in a layer above the smaller dots. (c) Spherical coordinate system used angle-dependent torque calculation.

Using the ground state potential, we find the eigenstates ψ at the Fermi energy using an approach described in Refs. 33 and 34. We evaluate the charge current and spin torque³⁵ from a Boltzmann distribution of the states (within the relaxation time approximation):

$$I = \frac{e^2 \tau}{\hbar(2\pi)^2} \int d\mathbf{k}_{\parallel} (v_{\mathbf{k}_{\parallel}}^R - v_{\mathbf{k}_{\parallel}}^L) E_x, \quad (1)$$

$$\Gamma = \frac{e\tau}{\hbar(2\pi)^2} \int d\mathbf{k}_{\parallel} (\mathbf{t}_{\mathbf{k}_{\parallel}}^R - \mathbf{t}_{\mathbf{k}_{\parallel}}^L) E_x, \quad (2)$$

$$\mathbf{t}_{\mathbf{k}_{\parallel}}^{R,L} = \int d\mathbf{r} \{ \psi_{\mathbf{k}_{\parallel}}^{R,L*}(\mathbf{r}) [\mathbf{S} \times \Delta(\mathbf{r})] \psi_{\mathbf{k}_{\parallel}}^{R,L}(\mathbf{r}) \}, \quad (3)$$

where τ is the lifetime, and \mathbf{k}_{\parallel} is the two-dimensional Bloch wave vector normal to the current direction (so that the resulting integral is one dimensional). $v_{\mathbf{k}_{\parallel}}^{(L,R)}$ is the state group velocity, \mathbf{S} is the spin operator, and $\Delta(\mathbf{r})$ is the spin-dependent exchange-correlation potential. The superscript R (L) refers to states with positive (negative) group velocity in the \hat{x} direction. The above expressions include a suppressed single sum over band indices. The resulting torque per current is independent of scattering time τ . Converting the one-dimensional transport integrals requires a finer mesh spacing ($dk = 0.044$ nm⁻¹) than needed for the ground state energy. While the torque varies strongly with the magnetization direction, the effective field only varies weakly. We present our results in terms of a scaled effective field:

$$H_R/J = \frac{\Gamma \cdot [\mathbf{M} \times (\hat{\mathbf{J}} \times \hat{\mathbf{z}})]}{|\mathbf{M} \times (\hat{\mathbf{J}} \times \hat{\mathbf{z}})|^2} \frac{d}{M_s I}, \quad (4)$$

where M_s is the computed magnetization density, d is the slab thickness, and J is the three dimensional current density. The result has units of field per bulk current density, a quantity commonly used to report experimental results.

Equation (3) captures some—but not all—contributions to the current-induced torque. In the language of Ref. 25, we

only include the odd torques, and hence neglect any intrinsic spin Hall effect in the Pt layers or at the interface. We also neglect effects from interband scattering on the torques³⁶ as well as higher order corrections due to momentum scattering that were considered in Refs. 21,22, and 24 for a Rashba model. Reference 25 shows that for Co/Pt, the even torque is dominated by the spin Hall effect and the interfacial contributions are negligible. We also neglect skew scattering that could also give a spin Hall effect. Thus, we only capture the current-induced torque related to the Rashba model and neglect all contributions from the spin Hall effect in the bulk of the Pt. Recent models of this system employing a Boltzmann model show that the Rashba and spin Hall effect torques are largely independent of each other.³⁷ We use the approach described here to focus on understanding the contribution to the current-induced torque from the spin-orbit coupling near the interface.

Our calculations are complementary to those of Ref. 25. Those calculations compute the torque for the magnetization parallel and antiparallel to the interface normal and consider the even and odd components. These are equivalent to the dampinglike and fieldlike torques. Their calculations include the spin Hall effect in the Pt and so describe the dampinglike torque that we neglect. Where the calculations can be compared, we find similar results. The reduced computational demands of our approach enable us to explore a wider range of systems, including different geometries and different magnetization orientations.

III. RESULTS

We first consider the important energy scales in the system: the spin-orbit coupling and the exchange spin splitting. Figure 2 shows the calculated bulk band structure of bulk Pt with and without spin-orbit coupling. The spin-orbit splittings are large at points of high symmetry: The spin-orbit splitting at $\mathbf{k} = 0$ of the Γ'_{25} band is on the order of 1 eV. For bulk hcp Co, we find an exchange splitting energy Δ of about 1 eV. We show below that the exchange splitting in the Co induces exchange splitting (and a small moment) in the Pt and that the spin-orbit coupling in the Pt induces a transverse moment in the Co. Of these proximity effects, the transverse

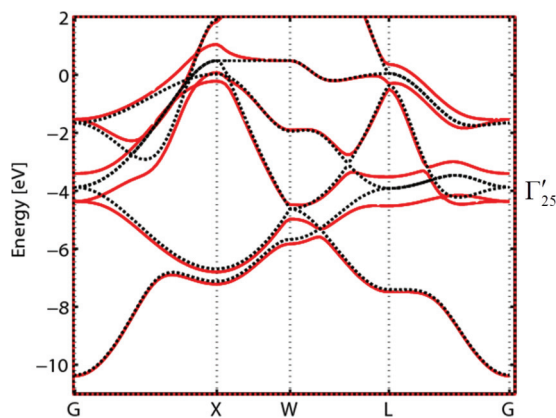


FIG. 2. (Color online) Band structure of bulk Pt. Solid lines: with spin-orbit coupling, dotted lines: without spin-orbit coupling.

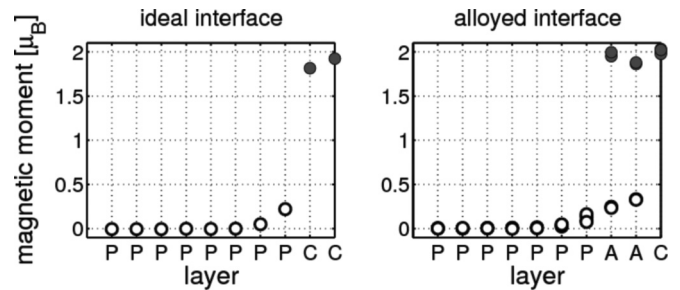


FIG. 3. Magnetic moment versus layer for (a) 8 layers of Pt (P) and 2 layers of Co (C), and (b) 8 layers of Pt and 2 alloyed (A) layers and 1 layer Co [see Fig. 2(b) for the alloy coordinates]. The four atomic moments in each layer are plotted individually (since the disordered interface has inequivalent atoms in each layer), where filled (open) symbols represent Pt (Co). The moments are oriented in the \hat{z} direction.

moment on the Co induced by the spin-orbit coupling in the Pt plays the dominant role in determining the current-induced torques.

The layer resolved magnetic moments are shown in Fig. 3(a). The induced moment on the interface Pt layer varies with the Co coverage, with values of 0.30, 0.22, and 0.25 μ_B for 1, 2, and 3 ML of Co, respectively. These values are similar to those found in previous calculations^{30,38,39} and to experimental measurements (Refs. 26, 40, and 41 measure a Pt interface moment of $\approx 0.2 \mu_B$, while Ref. 42 measures a moment of $\approx 0.6 \mu_B$). Figure 3(b) shows the moments in each layer for the disordered interface geometry showed in Fig. 1(b). The moments on the Pt atoms in the alloyed interface range from 0.25 to 0.4 μ_B . The importance of this proximity magnetization in the metal is an open question. In a recent experiment, a Au layer was placed between the Pt and the Co.¹¹ Au has a lower magnetic susceptibility and a much smaller induced moment. It is found that increasing the Au layer thickness reduces the offset in the current-domain wall velocity curves, which is explained by a reduction in the DM interaction. It is concluded that proximate magnetization plays a central role in one of the important spin-orbit coupling effects at the interface (the DM interaction).¹¹ On the other hand, our calculations suggest that the transverse spin in the Co induced by the Pt plays a more important role for the fieldlike torque, as we discuss at the end of this section.

Figure 4(a) shows the layer-resolved effective field per current for 1, 2, and 3 ML of Co (note the field is layer resolved, but the current is the layer averaged). The largest field (or largest torque) is on the Co atoms, although there is also torque present on the magnetized Pt layer. The effective field per current for various geometries are listed in Table I. Experimental values range from a high⁵ of $10^{-12} \text{ T m}^2/\text{A}$ to slightly above^{10,43} $10^{-14} \text{ T m}^2/\text{A}$, although the precise value is highly dependent on system details like layer thicknesses: Ref. 44 finds an order of magnitude difference in the current-induced effective field when the magnetic layer thickness changes from 1 to 1.2 nm. We also find the magnitude depends sensitively on coverage. Figure 4(b) shows the effective field for an alloyed interface. The total magnitude is decreased in all alloyed interfaces we have investigated, relative to the ideal

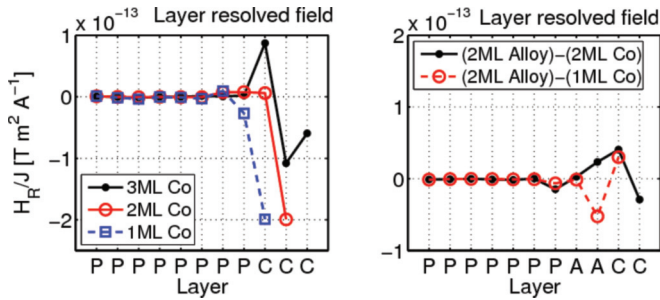


FIG. 4. (Color online) Layer resolved effective field per current density for (a) 1, 2, and 3 ML of Co with an ideal interface, and (b) 2 alloyed interfaces.

interface. The torques are again predominantly localized on the Co atoms, and they are nearly oppositely oriented for Co atoms in the alloy layer adjacent to the pure Pt. This cancellation is largely responsible for the decrease in the total current-induced torques. Note that our result for the 8-3 ML Pt-Co system is similar to that of Ref. 25, despite some slight differences in the structures used in the two calculations.

The torques are largely unchanged if we use hcp stacking for the Co layers (see Table I). They do change in calculations for larger Co-Pt and Co-Co interplane distance, but the trends with respect to Co coverage and alloying are similar. We highlight the trend that the torques are decreased for imperfect interfaces, and that these decreased values are in semiquantitative agreement with experiment.^{10,43}

It is interesting to compare the efficiency of current-induced torques resulting from interfacial spin-orbit coupling to the more conventional spin transfer torques present in noncollinear spin valves. In both cases, the torques are interfacial effects which are proportional to current density. The relevant quantity for the current-induced torque is therefore the torque per area per current density. Scaling this by μ_B/e results in a dimensionless efficiency. In spin valves, the spin transfer torque is equal to the flux of transverse spin, and the efficiency

TABLE I. Fieldlike torque for different film geometries. The first column gives the number of pure Pt layers, the number of alloy layers, and the number of pure Co layers. In the second and third columns, no “•” appears if the spin-orbit coupling (second) or exchange potential (third) has been set to zero. The two different structures considered for the 8-2-1 geometry are designated (a) and (b).

Structure	SO on Pt	Δ on Pt	H_R/J ($10^{-14} \text{ T m}^2/\text{A}$)
8-0-1	•	•	-22.4
8-0-2	•	•	-17.9
8-0-2	•		-19.5
8-0-2		•	-3.2
8-0-2(hcp)	•	•	-18.9
8-1-1	•	•	-11.1
8-2-1 (a)	•	•	-3.3
8-2-1 (a)	•		-3.9
8-2-1 (a)		•	2.9
8-2-1 (b)	•	•	-3.7
8-0-3	•	•	-7.7
8-2-2	•	•	-1.9

is approximately equal to the polarization of the current. We convert the effective fields of Table I into a torque per area by multiplying by γM_s , where γ is the gyromagnetic ratio and M_s is the two-dimensional magnetization density. The largest efficiency we find is 0.300 for the 8-0-2 system, while the smallest efficiency is 0.048 for the 8-2-2 system.

As noted above, our calculations include only the odd contribution to the torque, $\Gamma(\hat{\mathbf{M}}) = -\Gamma(-\hat{\mathbf{M}})$. This contribution is dominated by the fieldlike torque. For certain orientations of the magnetization, we also find a component of the torque perpendicular to the fieldlike torque, that is, in the direction of the dampinglike torque. The angular dependence of the dampinglike torque is given by $H_D(\mathbf{M})\{\hat{\mathbf{M}} \times [\hat{\mathbf{M}} \times (\hat{\mathbf{j}} \times \hat{\mathbf{z}})]\}$. The odd dampinglike torque we calculate has a prefactor H_D which is odd in \mathbf{M} . This dampinglike torque is a reactive torque, to be distinguished from the dissipative dampinglike torques due to spin Hall effect plus spin transfer. Figure 5(a) shows the angular dependence of the current-induced fields responsible for the fieldlike and the odd dampinglike torques. The left panels are for an ideal 8-2 ML Co-Pt system, and the right panels are for a disordered interface as shown in Fig. 1(b). For the Rashba model in the limit where the exchange potential is much larger than the spin-orbit coupling energy, the equivalent fields are independent of the magnetic orientation.¹⁵ However, when the exchange potential and spin-orbit coupling

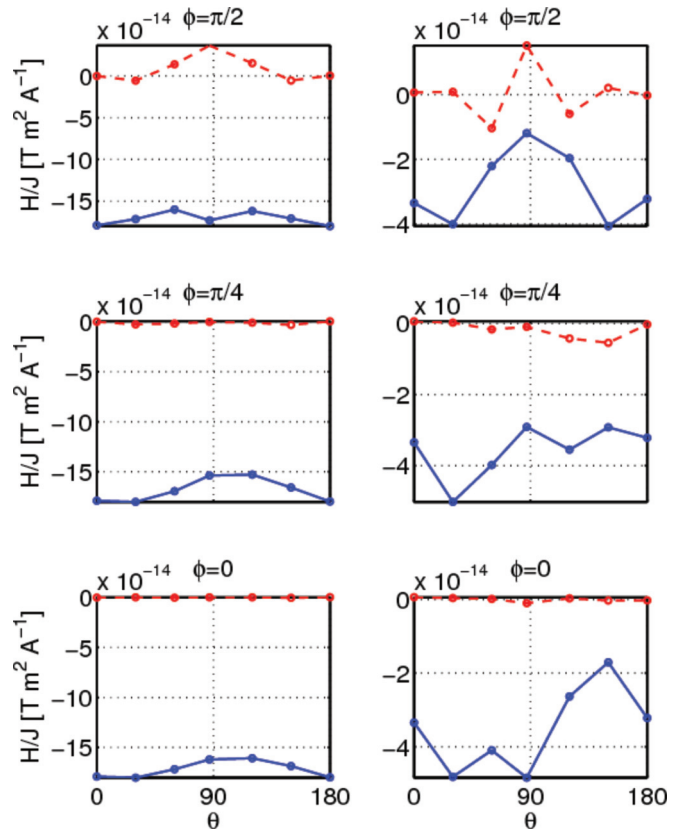


FIG. 5. (Color online) The angular dependence of the effective field (solid blue) and odd “damping field” (dashed red) magnitude per current density. The left panel is for 2 ML of Co with an ideal interface, while the right panel is for 2 layers of alloy + 1 layer Co. The angles are conventional spherical coordinates for the coordinate system of Fig. 1.

are similar in magnitude, the angular dependence of the fields found from the Rashba model is similar to that shown here.⁴⁵ Based on Fig. 5, we conclude that the simple Rashba model description of bilayers accounts reasonably well for many properties of the torque (at least for an ideal interface).

We next comment on the odd dampinglike torque calculated in our system. We first note that if a system is isotropic in the x - y plane, the odd torque is entirely fieldlike. This is because $(\mathbf{k} \times \mathbf{S}) \cdot \hat{\mathbf{z}}$ should remain invariant under rotations about the z axis. The eigenstates therefore have spin components S_x, S_z which are even functions of k_x , and S_y which is an odd function of k_x .⁴⁶ Forming a current-carrying distribution in the \hat{x} direction leads to a spin accumulation purely in the \hat{y} direction, yielding a fieldlike torque. However, the inequivalence of $+\hat{x}$ and $-\hat{x}$ directions of our lattice removes the symmetry constraints when the magnetization has a \hat{y} component, so that a spin accumulation of any direction is allowed by symmetry.⁴⁷ This in turn leads to both fieldlike and odd dampinglike torques. For real systems with disordered interfaces, we expect the in-plane direction to be relatively isotropic, so that the odd torque is primarily fieldlike (at least within the relaxation time approximation).

To further illustrate the similarities and differences of the system with simple Rashba model, we plot the states at the Fermi energy in Fig. 6. Despite the enormous complexity of the electronic structure, there are similarities to the Rashba model. This is shown in Figs. 6(c) and 6(d), which depict the spin structure of states near $\mathbf{k} = 0$. Note that the states on the circle with $|\mathbf{k}|a_0 = 0.09$ have a spin direction which varies to make $(\mathbf{k} \times \mathbf{S}) \cdot \hat{\mathbf{z}}$ positive. The symmetry of the Fermi surface and \mathbf{k} dependence of the spin follows from the system symmetry.⁴⁷ The current-induced torque arises when summing over a current carrying distribution of these states (recall the current to be in the \hat{x} direction). The sizable transverse moments of the states, shown in Figs. 6(c) and 6(d), are the result of the interaction of the Co orbitals with the spin-orbit potential localized on the Pt.

Summing over states leads to significant cancellation of the torques. We find that the average absolute value of torque from each state is about 10 to 100 times greater than the integrated total, depending on the specific system. As described in Ref. 49, this cancellation can be understood qualitatively in a tight-binding model, where different bands have different signs of orbital chirality $\pm(\mathbf{k} \times \mathbf{L}) \cdot \hat{\mathbf{z}}$.⁴⁸ The addition of spin-orbit coupling $\mathbf{L} \cdot \mathbf{S}$ then (roughly speaking) leads to alignment of the spin in the $\pm(\mathbf{k} \times \mathbf{S}) \cdot \hat{\mathbf{z}}$ direction, resulting in different signs of an effective Rashba parameter for different states.⁴⁹

We next attempt to identify the most important interface properties which determine the current-induced torque. A current-induced torque from a Rashba-like model requires the simultaneous presence of exchange splitting and spin-orbit coupling. It is not *a priori* obvious if the induced exchange present in the Pt is more or less important than the induced spin-orbit coupling in the Co.

The magnetic proximity effect is a dramatic example of the effect of hybridization between neighboring materials' orbitals. However, as discussed in Ref. 49, there is a similar energy splitting on the Co orbitals due to the interaction with the spin-orbit coupling in the Pt. This effect is not as obvious as

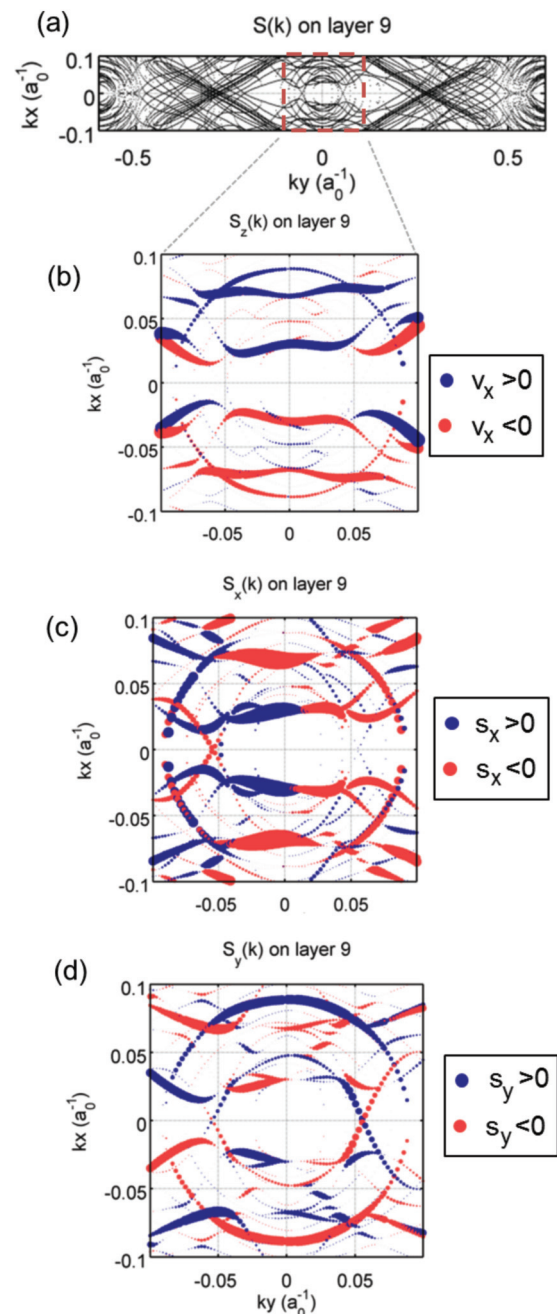


FIG. 6. (Color online) (a) Plot of states at the Fermi level versus wave vector. (b) Zoom in of states near the zone center. The dark blue (light red) color indicates states with positive (negative) group velocity in the x direction. The dot size of each state is proportional to the magnitude of the state's z component of spin on the interface Co layer. (c) The x component of spin on the interface Co layer. The magnitude of each state's spin is proportional to the dot size, and the colors (shading) indicate the sign of S_x . (d) The same plot for the y component of each state's spin. The torque on the interface Co layer contributed by each state is proportional to the in-plane spin component for that state.

the magnetic proximity effect for two reasons: The Co levels with which Pt hybridize are pure spin states, which leads to appreciable spin splitting for all Pt states, and a macroscopic magnetization in the Pt interface layer. On the other hand, the

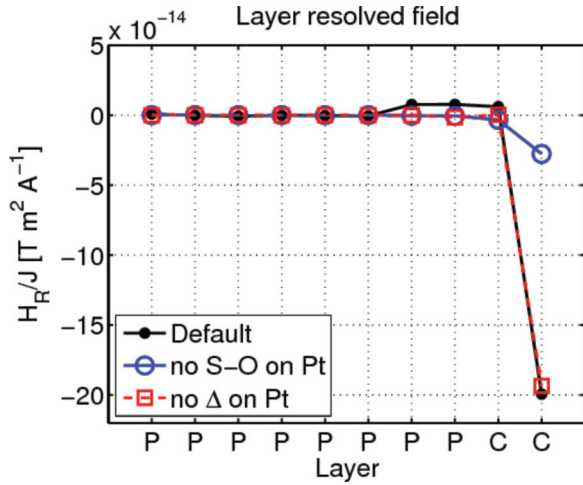


FIG. 7. (Color online) Layer resolved torque for 8 layer Pt and 2 layer Co system. “Default” refers to the system with full exchange and spin-orbit coupling. The other torques are calculated by removing the specified potential from the Pt atoms, as described in the text.

eigenstates of the atomic spin-orbit potential $\mathbf{L} \cdot \mathbf{S}$ are those of the total angular momentum operator $\mathbf{J} = \mathbf{L} + \mathbf{S}$. \mathbf{J} is not a good quantum number in the symmetry broken crystal field, so the Pt states with which Co hybridize generally do not directly reflect the spin orbit potential. This obscures the effect of the Pt spin-orbit on the levels in the Co. Despite being less “obvious” in this way, the proximate effect of the spin-orbit coupling is quite important, as we show next.

To determine the role of magnetic proximity effect, we remove the exchange splitting on the Pt atoms from the ground state Hamiltonian, and the resulting current-induced torques are calculated as described in Sec. II. To determine the role of the spin-orbit coupling proximity effect, we remove the spin-orbit potential from the Pt atoms, perform a new ground state calculations, and calculated the current-induced torques. (We find that removing the Pt spin-orbit potential from the initial ground state and calculating the current-induced torques *without* performing a new ground state calculations yields very similar results.)

Figure 7 shows the results for the ideal interface. The current-induced effective field is nearly unchanged when the Pt magnetization is removed, and greatly diminished when the Pt spin-orbit coupling is removed. We conclude that the spin-orbit in the Pt is the main agent behind the total torque. We additionally repeat this calculation for an alloyed system, with the layer and atom-resolved torques shown in Fig. 8. A similar scenario holds in this case. [Note however that the magnitude of the *total* torques are not so different in the alloyed case

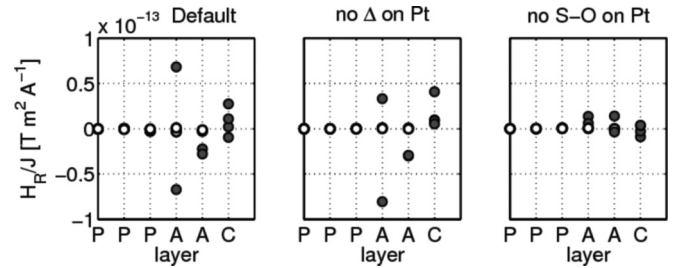


FIG. 8. Similar plot as Fig. 7, but with an alloyed interface. The individual torques on the four atoms of each layer are shown (the torques from the bottom five Pt layers are omitted from the plot, as they vanish). Open (filled) circles represent Pt (Co).

(see Table I) when we remove the spin-orbit from the Pt; this is due to the significant cancellations that occur when adding the contributions from all the states in the default system.] It is instructive to evaluate the average absolute value of the torque from all states for these different scenarios. We find the torques are nearly unchanged for no magnetization on Pt, while they are about 5 times smaller when the spin-orbit is removed from the Pt. To rationalize this result, we note that the exchange splitting in the Pt is 10 times smaller than in the Co. On the other hand, the transverse spin density is 3 times smaller in the Co than in the Pt. These properties of the states indicate that the Pt spin-orbit potential is the primary source of the overall torque.

IV. CONCLUSION

In summary, we performed first-principles calculations of the fieldlike current-induced torque on a series of Co-Pt bilayers, and from this we conclude that: (1) the torque is very sensitive to system details, such as Co coverage. This is consistent with experimental data, and the general magnitude of the calculated effective fields is similar to the experimental values. (2) The angular dependence of the torque is very similar to that predicted by the simple 2D Rashba model for an ideal interface, but more complicated for alloyed interfaces. (3) The primary source of the torque is derived from the spin-orbit coupling localized on the Pt interface atoms, which affects the nonequilibrium spin density in the Co interface layer, and drives the current-induced torques. The extent to which the trends revealed by the first-principles calculations can be made more revealing in simpler models is a question for future work. In addition, this approach may be used to screen different materials combinations in order to anticipate which materials may show the strongest effect.

¹D. C. Ralph and M. D. Stiles, *J. Magn. Magn. Mater.* **320**, 1190 (2008).

²J. A. Katine and E. E. Fullerton, *J. Magn. Magn. Mater.* **320**, 1217 (2008).

³W.-G. Wang, M. Li, S. Hageman, and C. L. Chien, *Nat. Mat.* **11**, 64 (2011).

⁴D. Chiba, M. Sawicki, Y. Nishitani, Y. Nakatani, F. Matsukura, and H. Ohno, *Nature (London)* **455**, 515 (2008).

⁵I. M. Miron, G. Gaudin, S. Auffret, B. Rodmacq, A. Schuhl, S. Pizzini, J. Vogel, and P. Gambardella, *Nat. Mat.* **9**, 230 (2010).

- ⁶I. M. Miron, T. Moore, H. Szabolcs, L. D. Buda-Prejbeanu, S. Auffret, B. Rodmacq, S. Pizzini, J. Vogel, M. Bonfim, A. Schuhl, and G. Gaudin, *Nat. Mater.* **10**, 419 (2011).
- ⁷I. M. Miron, K. Garello, G. Gaudin, P.-J. Zermatten, M. V. Costache, S. Auffret, S. Bandiera, B. Rodmacq, A. Schuhl, and P. Gambardella, *Nature (London)* **476**, 189 (2011).
- ⁸L. Liu, O. J. Lee, T. J. Gudmundsen, D. C. Ralph, and R. A. Buhrman, *Phys. Rev. Lett.* **109**, 096602 (2012).
- ⁹K. Ando, S. Takahashi, K. Harii, K. Sasage, J. Ieda, S. Maekawa, and E. Saitoh, *Phys. Rev. Lett.* **101**, 036601 (2008).
- ¹⁰J. Kim, J. Sinha, M. Hayashi, M. Yamanouchi, S. Fukami, T. Suzuki, S. Mitani, and H. Ohno, *Nat. Mat.* **12**, 240 (2013).
- ¹¹K.-S. Ryu, L. Thomas, S.-H. Yang, and S. Parkin, *Nat. Nanotech.* **8**, 527 (2013).
- ¹²S. Emori, U. Bauer, S.-M. Ahn, E. Martinez, and G. S. D. Beach, *Nat. Mat.* **12**, 611 (2013).
- ¹³X. Fan, J. Wu, Y. P. Chen, M. J. Jerry, H. W. Zhang, and J. Q. Xiao, *Nat. Commun.*, **4**, 1799 (2013).
- ¹⁴L. Liu, C.-F. Pai, Y. Li, H. W. Tseng, D. C. Ralph, and R. A. Buhrman, *Science* **336**, 555 (2012).
- ¹⁵A. Manchon and S. Zhang, *Phys. Rev. B* **78**, 212405 (2008).
- ¹⁶I. E. Dzyaloshinskii, *Sov. Phys. JETP* **5**, 1259 (1957).
- ¹⁷T. Moriya, *Phys. Rev.* **120**, 91 (1960).
- ¹⁸K.-W. Kim, H.-W. Lee, K.-J. Lee, and M. D. Stiles, *Phys. Rev. Lett.* **111**, 216601 (2013).
- ¹⁹A. Thiaville, S. Rohart, É. Jué, V. Cros, and A. Fert, *Europhys. Lett.* **100**, 57002 (2012).
- ²⁰The choice of vector components along which to project the torque is arbitrary, but the conventional choice described here is convenient for these systems. There can be additional angular dependence of the torque component's magnitudes, as we show in Fig. 5.
- ²¹D. A. Pesin and A. H. MacDonald, *Phys. Rev. B* **86**, 014416 (2012).
- ²²X. Wang and A. Manchon, *Phys. Rev. Lett.* **108**, 117201 (2012).
- ²³E. van der Bijl and R. A. Duine, *Phys. Rev. B* **86**, 094406 (2012).
- ²⁴K.-W. Kim, S. M. Seo, J. Ryu, K.-J. Lee, and H.-W. Lee, *Phys. Rev. B* **85**, 180404 (2012).
- ²⁵F. Freimuth, S. Blügel, and Y. Mokrousov, [arXiv:1305.4873](https://arxiv.org/abs/1305.4873).
- ²⁶S. Ferrer, J. Alvarez, E. Lundgren, X. Torrelles, P. Fajardo, and F. Boscherini, *Phys. Rev. B* **56**, 9848 (1997).
- ²⁷E. Lundgren, B. Stanka, M. Schmid, and P. Varga, *Phys. Rev. B* **62**, 2843 (2000).
- ²⁸Large supercell calculations [of cell size up to $(7 \times 7)X/(8 \times 8)$ Co, X = Au, Pt] with a fully relaxed surface structure in the absence of spin-orbit coupling show that the magnetic moment carried by the Co layer is decreased by about 20% for realistic interfaces, relative to highly strained, idealized interfaces.²⁹ We therefore suspect that the ideal interfaces will lead to an overestimation of the current-induced torque relative to more realistic interface structures (which is also consistent with the disordered interface calculations presented here).
- ²⁹S. Grytsyuk and U. Schwingenschlögl, *Phys. Rev. B* **88**, 165414 (2013).
- ³⁰R. Wu, C. Li, and A. J. Freeman, *J. Magn. Magn. Mater.* **99**, 71 (1991).
- ³¹J. P. Perdew and A. Zunger, *Phys. Rev. B* **23**, 5048 (1981).
- ³²L. Fernández-Seivane, M. A. Oliveira, S. Sanvito, and J. Ferrer, *J. Phys. Cond. Mat.* **18**, 7999 (2006).
- ³³J. Taylor, H. Guo, and J. Wang, *Phys. Rev. B* **63**, 245407 (2001).
- ³⁴J. Taylor, Ph.D. thesis, McGill University, 2000.
- ³⁵A. Núñez and A. H. MacDonald, *Solid State Commun.* **139**, 31 (2006).
- ³⁶H. Kurebayashi, Jairo Sinova, D. Fang, A. C. Irvine, J. Wunderlich, V. Novák, R. P. Campion, B. L. Gallagher, E. K. Vehstedt, L. P. Zarbo, K. Výborný, A. J. Ferguson, and T. Jungwirth, [arXiv:1306.1893](https://arxiv.org/abs/1306.1893).
- ³⁷P. M. Haney, H.-W. Lee, K.-J. Lee, A. Manchon, and M. D. Stiles, *Phys. Rev. B* **87**, 174411 (2013).
- ³⁸G. Moulas, A. Lehnert, S. Rusponi, J. Zabloudil, C. Etz, S. Ouazi, M. Etzkorn, P. Bencok, P. Gambardella, P. Weinberger, and H. Brune, *Phys. Rev. B* **78**, 214424 (2008).
- ³⁹A. Lehnert, S. Dennler, P. Błoński, S. Rusponi, M. Etzkorn, G. Moulas, P. Bencok, P. Gambardella, H. Brune, and J. Hafner, *Phys. Rev. B* **82**, 094409 (2010).
- ⁴⁰J. Geissler, E. Goering, M. Justen, F. Weigand, G. Schütz, J. Langer, D. Schmitz, H. Maletta, and R. Mattheis, *Phys. Rev. B* **65**, 020405(R) (2001).
- ⁴¹S. M. Valvidares, T. Schroeder, O. Robach, C. Quirós, T.-L. Lee, and S. Ferrer, *Phys. Rev. B* **70**, 224413 (2004).
- ⁴²M. Suzuki, H. Muraoka, Y. Inaba, H. Miyagawa, N. Kawamura, T. Shimatsu, H. Maruyama, N. Ishimatsu, Y. Isohama, and Y. Sonobe, *Phys. Rev. B* **72**, 054430 (2005).
- ⁴³K. Garello, I. M. Miron, C. O. Avci, F. Freimuth, Y. Mokrousov, S. Blügel, S. Auffret, O. Boulle, G. Gaudin, and P. Gambardella, *Nat. Nanotech.* **8**, 587 (2013).
- ⁴⁴T. Suzuki, S. Fukami, N. Ishiwata, M. Yamanouchi, S. Ikeda, N. Kasai, and H. Ohno, *Appl. Phys. Lett.* **98**, 142505 (2011).
- ⁴⁵K.-J. Lee *et al.* (unpublished).
- ⁴⁶The relevant symmetry operation is reflection in the x - y plane + time reversal.
- ⁴⁷If the magnetization is in the x - z plane, the system is invariant under operations of reflection about the x - z plane (taking $y \rightarrow -y$) followed by time reversal. This implies degenerate states at (k_x, k_y) and $(-k_x, k_y)$, with equal S_x and S_z , and opposite S_y , yielding exclusively a fieldlike torque. A similar argument can not be made for magnetization in the y - z plane, because the lattice is not invariant under $x \rightarrow -x$.
- ⁴⁸S. R. Park, C. H. Kim, J. Yu, J. H. Han, and C. Kim, *Phys. Rev. Lett.* **107**, 156803 (2011).
- ⁴⁹J.-H. Park, C. H. Kim, H.-W. Lee, and J. H. Han, *Phys. Rev. B* **87**, 041301(R) (2013).